

Energy spectrum of the Burgers and KPZ equations with correlated noise

Mahendra K. Verma *

*Department of Physics, Indian Institute of Technology,
Kanpur – 208016, INDIA
(December 2, 2024)*

We numerically calculate the energy spectrum of the one-dimensional Burgers and KPZ equations with correlated noise. We have used pseudo-spectral method for our analysis. When ρ of the KPZ noise variance (variance $\propto k^{-2\rho}$) exceeds $5/2$, large shocks appear in the velocity profile leading to $\langle |u(k)|^2 \rangle \propto k^{-2}$. However, for $0 \leq \rho \leq 1$, the profile is dominated by noise, and the spectrum $\langle |h(k)|^2 \rangle$ of the corresponding KPZ equation is in close agreement with Medina et al.'s renormalization group predictions. In the intermediate range $1 < \rho < 5/2$, both noise and well-developed shocks are seen, consequently the exponents slowly vary from RG regime ($\rho < 1$) to a shock-dominated regime ($\rho > 5/2$). We also calculate the energy cascade rates for all ρ and find a constant flux for all ρ above 1.5.

PACS Number: 47.27.Cn, 47.54.+r, 68.10.-m, 02.50.Ey

I. INTRODUCTION

Stochastic Burgers equation has been studied extensively because of its close connection with the Navier-Stokes equation. Recently it has been found that Burgers equation with correlated noise shows intermittency [1–3], however these calculations have been done for specific degrees of noise correlation. In this paper and paper II [4] we vary the applied noise from uncorrelated regime to strongly correlated regime and study extensively the energy spectrum and the intermittency exponents. Specifically, paper I deals with the numerical calculation of energy spectrum and energy transfer rates, and paper II deals with the computation of q th order structure functions and the probability distribution functions of u and du/dx , where $u(x, t)$ is the velocity function appearing in the Burgers equation.

The one-dimensional Burgers equation is

$$\frac{\partial u}{\partial t} + \lambda u \frac{\partial u}{\partial x} = \nu \frac{\partial^2 u}{\partial x^2} + \zeta, \quad (1.1)$$

where u is the velocity field, λ is the strength of the nonlinear term ($\lambda = 1$ in the standard equation), ν is the viscosity, and ζ is the noise. We assume that the noise $\zeta(k, t)$ is gaussian ($\zeta(k)$ is the Fourier transform of $\zeta(x)$), and in Fourier space follows distribution

$$\langle \zeta(k, t) \zeta(k', t') \rangle = 2Dk^{-2\sigma} (2\pi)^2 \delta(k + k') \delta(t - t'). \quad (1.2)$$

Kida [5], Gotoh [6], and Bouchaud et al. [7] have solved the noiseless Burgers equation ($\zeta = 0$) exactly in limit of large time t and zero viscosity [8,9]. The solution is a linear profile with sharp discontinuities, which are called shocks. It has been found from this solution that the energy spectrum $\langle |u(k)|^2/2 \rangle \propto k^{-2}$ ($u(k)$ is the Fourier transform of $u(x)$); the spectrum k^{-2} essentially comes from the shocks. We will show in this paper that the shocks are also seen in the Burgers equation with large noise correlations ($\sigma > 3/2$). As a consequence, the energy spectrum exponent is again close to 2 for $\sigma > 3/2$.

The Kardar-Parisi-Zhang (KPZ) equation, which describes a generic set of surface growth phenomena, is closely related to the Burgers equation. The replacement of u by $-\partial h/\partial x$ in the Burgers equation yields KPZ equation:

*email:mkv@iitk.ac.in

$$\frac{\partial h}{\partial t} = \frac{\lambda}{2} \left(\frac{\partial h}{\partial x} \right)^2 + \nu \frac{\partial^2 h}{\partial x^2} + f(\mathbf{x}, t), \quad (1.3)$$

where $h(x, t)$ is the height of the surface profile at position x and time t , λ is the strength of the nonlinearity, ν is the diffusion coefficient, and f is the forcing function. We again assume that the noise $f(k, t)$ is gaussian, and in Fourier space follows distribution

$$\langle f(k, t)f(k', t') \rangle = 2Dk^{-2\rho} (2\pi)^2 \delta(k + k')\delta(t - t'). \quad (1.4)$$

It can be easily shown from the above equations that $|u(k)|^2 = k^2|h(k)|^2$ and $\sigma = \rho - 1$. It can be easily shown using these relationships that the spectrum of the noiseless KPZ equation $\langle |h(k)|^2 \rangle = \langle |u(k)/k|^2 \rangle \propto k^{-4}$.

Eq. (1.3) has been solved by Kardar-Parisi-Zhang [10] for $\rho = 0$ and by Medina et al. [11] for $0 < \rho \leq 1$ using renormalization group analysis. They have calculated the roughening exponents χ and β , which characterize the dynamical properties of the equation, e.g., $\langle |h(k)|^2 \rangle \propto k^{-2\chi-1}$. The RG analysis is not applicable beyond $\rho = 1$. Using the connection of the Burgers equation with the KPZ equation, the dynamical exponents of the Burgers equation is also automatically solved for this set of ρ . Recently, Chattopadhyay and Bhattacharjee [12] have applied mode coupling scheme and obtained the same exponents for KPZ equation for $\rho \leq 1$. For $\rho > 1$ Chattopadhyay and Bhattacharjee [12] find that $\chi/\beta = 1$.

Chekhlov and Yakhot [1], and Hayot and Jayaprakash [3] numerically solved the Burgers equation with correlated noise for a range of ρ . For $\rho = 3/2$, Chekhlov and Yakhot [1] obtained Kolmogorov's energy spectrum, i.e., $|u(k)|^2 \propto k^{-5/3}$. They argued that the constancy of energy flux is the reason for Kolmogorov's spectrum in the noisy Burgers equation with $\rho = 3/2$. Hayot and Jayaprakash [3] have numerically calculated the energy spectrum for $0 \leq \rho \leq 3/2$. They find that shocks play an important in the determination of the exponents for $\rho > 1$. In this paper we have extended the range of ρ beyond $3/2$. As mentioned earlier, we find that for large ρ the spectrum is essentially determined by the shocks.

The roughening exponents for KPZ equation χ and β have also been calculated by Zhang by replica method [13] and by Hentschel and Family using scaling arguments [14], and they find a close agreement with the results of Medina et al. [11]. Numerically, Peng et al. [15] have calculated the exponents χ and β using finite-difference method, and Amar et al. [16] and Meakin and Jullien [17,18] have calculated using lattice simulations. Their results are somewhat consistent with the RG predictions with large error bars.

The energy cascade rate is one of the important quantities of interest in the statistical theory of turbulence. In this paper we have computed the energy flux of the Burgers equation for $0 \leq \rho < 7$. We find a constant flux for all ρ beyond 1.5. In our simulation we also varied the values of the parameters (ν, λ, D) and analyzed its effects. We find that there are interesting crossover from KPZ to Edward Wilkinson (EW) equation depending on the values of the parameter. These crossover results are reported in the Appendix.

The outline of the paper is as follows: In section 2 we restate the earlier results regarding the energy spectrum for the noiseless Burgers, then use that result to derive the spectrum for KPZ equation. In section 3 and 4 we discuss our simulation method and results respectively. Sections 5 contains discussions and conclusions. In Appendix A we discuss the effects of variations of the parameters on the spectral indices. Appendix B contains a preliminary discussion on the calculation of exponents when both structures and noise are present.

II. EXPONENTS OF NOISELESS BURGERS AND KPZ EQUATION

We briefly discuss the exponents of the noiseless Burgers and KPZ equation because they will be compared with the exponents obtained for large ρ s. This is the restatement of the earlier results by Kida [5], Gotoh [6], and Bouchaud et al. [7]. The second order structure function of the Burgers equation, defined as $\langle |u(x+r) - u(x)|^2 \rangle$, has been calculated as

$$S_2(r) \approx \left(\frac{r}{t} \right)^2 + \frac{r}{L} \sum_i (\mu_i)^2, \quad (2.1)$$

where μ_i is the shock strength (defined as the velocity difference across the shock) of the i th shock, and L is the system size. The second term of the equation, which is due to the discontinuities at the shocks, dominates the first term for small r .

We can obtain the energy spectrum $E^u(k) = \langle |u(k)|^2/2 \rangle$ by taking the Fourier transform of the above function. Clearly,

$$\langle u(x+r)u(x) \rangle = \langle u^2 \rangle - \frac{1}{2}S_2(r). \quad (2.2)$$

Therefore,

$$\begin{aligned} E(k) &= \frac{1}{L} \int_{-\infty}^{\infty} 1/2 \langle u(x+r)u(x) \rangle \exp(-ikr) dr \\ &= \delta_{k,0} \frac{\langle u^2 \rangle}{2} + \frac{1}{2Lt^2} \frac{d^2 \delta_{k,0}}{dk^2} + (Lk)^{-2} \sum_i \mu_i^2. \end{aligned} \quad (2.3)$$

Note that the Fourier transform of r^2 is $d^2 \delta_{k,0}/dk^2$ [19]. Hence, the noiseless Burgers equation has energy spectrum $E^u(k) \propto k^{-2}$ for $k > 0$.

A point is in order here. Tatsumi and Kida [9] showed that the number of shock fronts decrease with t as $t^{-\gamma}$, where $0 \leq \gamma < 1$. Hence in the asymptotic state, there will be only several shocks, and the distance between the shock fronts will be of the order of box size. Hence r can be of the order of the system length in the asymptotic state.

Using the fact that $u(x,t)$ of Burgers equation is related to $h(x,t)$ by $u = -\partial h/\partial x$, we can easily solve the noiseless KPZ equation. The height $h(x,t) = -\int^x u(x',t) dx'$ will be

$$h(x,t) = \begin{cases} -\frac{x^2}{2t} + \frac{\eta_i}{t} (x - \xi_i) & \text{for } \frac{1}{2}(\xi_{i-1} + \xi_i) < x < \xi_i \\ -\frac{x^2}{2t} + \frac{\eta_{i+1}}{t} (x - \xi_i) & \text{for } \xi_i < x < \frac{1}{2}(\xi_i + \xi_{i+1}), \end{cases} \quad (2.4)$$

where ξ_i is the position of the i th shock, and η_i is the zeros of $u(x)$. In Fig. 1 we have shown $h(x,t)$ along with $u(x,t)$. After some algebra we can obtain the second-order structure function $T_2(r)$ for KPZ equation as

$$\begin{aligned} T_2(r) &\approx \frac{1}{3L} \left(\frac{r}{t}\right)^2 \sum_i [(\eta_{i+1} - \xi_{i+1})^3 - (\eta_{i+1} - \xi_i)^3] \\ &\quad + \frac{1}{3L} \left(\frac{r}{t}\right)^2 r \sum_i \frac{[(\eta_{i+2} - 2\xi_{i+1})^3 - (\eta_{i+1} - 2\xi_{i+1})^3]}{(\eta_{i+2} - \eta_{i+1})}. \end{aligned} \quad (2.5)$$

The solution of KPZ equation has cusps at the positions where shocks appear in Burgers equation. These cusps yield contributions proportional to r^3 , hence, to a leading order, $T_2(r) \propto r^2$. Note that any smooth continuous curve also has $T_2(r) \propto r^2$ because $h(x+r) - h(x) \approx h'r$ for small r .

The Fourier transform of the above equation yields

$$E^h(k) = \delta_{k,0} \frac{\langle h^2 \rangle}{2} + B \frac{d^2}{dk^2} \delta_{k,0} + \frac{C}{(Lt)^2} k^{-4}, \quad (2.6)$$

where B and C are constants [19]. Hence for $k > 0$, we obtain $E^h(k) \propto k^{-4}$ for the noiseless KPZ equation.

Most papers in the past implicitly assume that if $T_2(r) \propto r^{2\chi}$, then $E^h(k)$ should be proportional to $k^{-2\chi-1}$. Clearly this does not hold for the noiseless KPZ equation (check: $\chi = 1$, but $E^h(k) \propto k^{-4}$). This apparent contradictions, which also occurs for $\rho > 1$, can be resolved using the following arguments.

Suppose $E(k) = Ak^{-2\chi-1}$ ($\chi > 0$), where A is a constant. Clearly $\langle u(x+r)u(x) \rangle = FT[E(k)]$ is divergent. However, the second-order structure function $S_2(r)$ is convergent and is given by

$$\begin{aligned} S_2(r) &= \frac{1}{L} \int_0^L dx \langle |u(x+r) - u(x)|^2 \rangle \\ &= 16 \int_0^\infty dk E(k) \sin^2(kr/2) \\ &= 16 \int_0^\infty dk A k^{-2\chi-1} \sin^2(kr/2). \end{aligned} \quad (2.7)$$

We are interested in the leading order behaviour of $S_2(r)$ for small r . When $\chi < 1$, the above integral converges, and

$$\begin{aligned} S_2(r) &\propto 16Ar^{2\chi} \int_0^\infty ds s^{-2\chi-1} \sin^2(s) \\ &\approx AC_1 r^{2\chi}, \end{aligned} \quad (2.8)$$

where C_1 is a dimensionless constant. When $\chi > 1$, the integral diverges from below (small k). However, we can cure this divergence by choosing the lower limit of the integral to be $2\pi/L$. Hence,

$$\begin{aligned}
S_2(r) &\propto 16A \int_{2\pi/L}^{\infty} dk k^{-2\chi-1} (kr/2)^2 \\
&\approx AC_2(r/L)^2 L^{2\chi},
\end{aligned}
\tag{2.9}$$

where C_2 is a constant.

Hence, when $\chi < 1$, $E(k) \propto k^{-2\chi-1}$ and $S_2(r) \propto r^{2\chi}$ as expected, however when $\chi > 1$, $E(k) \propto k^{-2\chi-1}$ and $S_2(r) \propto r^2$. This analytical results are seen in our numerical simulations to be described below.

III. SIMULATION METHOD

Our calculations in this paper have been done using direct numerical simulations based on pseudo-spectral method. This method, commonly used in turbulence simulations, is expected to perform better than finite difference scheme because the derivatives can be calculated exactly in the spectral method [20]. The finite difference scheme was adopted by Moser et al. [21] and Peng et al. [15] in their simulation of KPZ equation for $\rho \leq 1$.

We solve the KPZ equation in one dimension. The details of the simulation are as follows. A box of size 2π is discretized into $N = 1024$ divisions. The KPZ equation is solved in Fourier space. However, to compute the nonlinear term, we go to real space, perform multiplication, then again come back to Fourier space. We time advance the Fourier components $h(k, t)$ using Adam Bashforth time marching procedure with flat surface as an initial condition. Two-third rule is used to remove aliasing [20]. For details of the simulation refer to Canuto et al. [20] and Verma et al. [22]. In our simulation we also add hyperviscosity term ($\kappa \nabla^4 h$) to the KPZ equation to damp the large wavenumber modes strongly. The hyperviscosity term does not affect the intermediate scales which is of our interest [22]; this is because the $\nabla^4 h$ and higher order derivative terms are irrelevant in the renormalization group sense (cf. Barabasi and Stanley [23] and references therein).

In our simulation we take ν and κ to be very small. Note that large ν correspond to Edward-Wilkinson (EW) equation. The dimensionless parameters used in our simulations are

$$\begin{aligned}
\lambda &= 1.0, \\
\nu &= 10^{-5}, \\
\kappa &= 10^{-6}, \\
(2\pi)^2 D &= 10^{-3}, \\
dt &= 1/2000
\end{aligned}
\tag{3.1}$$

with one exception. For $\rho = 0$, we choose $\lambda = 0.1$ for the stability of the code. In the Appendix A we have varied values of the parameters ν and D and shown crossover from KPZ behaviour to EW equation.

The values of ρ used in our simulation are 0.0, 0.15, 0.25, 0.40, 0.50, 0.75, 1.0, 1.5, 2.0, 3.0, and 7.0. We have time evolved the equation till 15 nondimensional time units. We find that the system reaches saturation in approximately 8 to 10 time units (refer to Fig. 2). As a reference, the time units 2π correspond to one eddy turn over time in fluid turbulence. For ensemble averaging, we have performed average over 100 samples starting with different random seeds for noise. We have used *ran1* of numerical recipes [24] as our random number generator. Each computer run for 15 time units and 100 samples takes approximately 7 hours on a Pentium machine (150 MHz).

We have calculated χ and β using the simulation data. The ensemble average $\langle . \rangle$ have been obtained by taking averages over 100 runs. The width $\langle \sum_x h^2(x)/N \rangle$ grows as a power law in time, i.e., $W(L, t) \propto t^\beta$, in the early stages of growth. We obtain β by fitting a straight line in *log-log* plot of $W(L, t)$ vs. t over a range of $t = 0.0 : 2.5$ (see Fig. 2 for $\rho = 0$). The other exponent χ is obtained from the asymptotic $\langle |h(k, t)|^2 \rangle$ averaged over 100 runs. A powerlaw fit for $\langle |h(k)|^2 \rangle$ over $k = 10 : 80$ at $t = 15$ yields χ ($|h(k)|^2 \propto k^{-2\chi-1}$). In Fig. 3 we plot $|h(k)|^2$ vs. k for $\rho = 0, 1, 1.5$, and 3. The lines of best fit are also shown in the Figure. The computed values of the exponents are listed in Table 1. Our estimate of the error in the exponent is roughly 0.05.

In the following section we will describe our simulation results for various degrees of noise correlations, i.e., for different ρ s.

IV. SIMULATION RESULTS

The parameter range of ρ can be divided in three regions: (a) $0 \leq \rho \leq 1$, (b) $1 \leq \rho \leq 5/2$, and (c) $\rho > 5/2$. The range $0 \leq \rho \leq 1$ comes naturally from the region of applicability of the RG calculations of Medina et al. [11]. The

value $5/2$ comes from the behaviour of real-space noise-noise correlation. The noise spectrum $|\zeta(k)|^2$ is proportional to $k^{2-2\rho}$. Using this we can derive the noise-noise correlation as

$$\langle \zeta(x, t) \zeta(x', t) \rangle \sim \begin{cases} B_0 \delta(r) & \text{for } \rho = 1 \\ B_1 - C_1 r^{2\rho-3} & \text{for } 1 \leq \rho \leq 3/2 \\ B_2 - C_2 \log(r) & \text{for } \rho = 3/2 \\ B_3 - C_3 |x - x'|^{2\sigma-1} & \text{for } \rho \leq 5/2 \\ B_4 - C_4 r^2 L^{2\sigma-3} & \text{for } \rho > 5/2 \end{cases} \quad (4.1)$$

where L is the length of the system, and B_i and C_i are constants. For $0 \leq \rho \leq 1$, $|\zeta(k)|^2 \rightarrow \infty$, hence, $\langle \zeta(x, t) \zeta(x', t) \rangle$ is not defined in this regime. However, Kardar et al. [10] and Medina et al. [11] have solved the KPZ equation for this regime using $|f(k)|^2$ which is well defined for large k .

It can be deduced from the above discussion that the noise-noise correlation increases with the increase of ρ till $\rho = 5/2$. After $\rho = 5/2$, the correlation is proportional to $1 - Cr^2$ for all ρ . Therefore, it is expected that the $h - h$ and $u - u$ correlation would increase with the increase of ρ till $5/2$, beyond which the behaviour is expected to be somewhat similar. Keeping this in mind we have divided the ρ range beyond 1 in two regions: (b) $1 \leq \rho \leq 5/2$, and (c) $\rho > 5/2$. Well defined shocks develop in the parameter range (c) due to the large noise-noise correlation, and these shocks determine the exponents. In the intermediate parameter range (b), the exponent changes slowly from RG dominated values to shock dominated values. The details are given below.

A. $0 \leq \rho \leq 1$

In Table 1 we have listed our numerical values of χ_{KPZ} and β_{KPZ} . For comparison we also list the predicted values of Medina et al. [11] below

$$\chi = \begin{cases} \frac{1}{2} & \text{for } 0 \leq \rho \leq \frac{1}{4} \\ \frac{1}{3} + \frac{2}{3}\rho & \text{for } 0 \leq \rho \leq \frac{1}{4} \end{cases} \quad (4.2)$$

and

$$\beta = \begin{cases} \frac{1}{3} & \text{for } 0 \leq \rho \leq \frac{1}{4} \\ \frac{1+2\rho}{5-2\rho} & \text{for } 0 \leq \rho \leq \frac{1}{4} \end{cases} \quad (4.3)$$

Medina et al.'s results are based on RG scheme that breaks down beyond $\rho = 1$.

We compute χ_{KPZ} by a straight line fit to the log-log plot of $\langle |h(k)|^2 \rangle$ over $k = 10 : 80$ at $t = 15$ ($|h(k)|^2 \propto k^{-2\chi-1}$) (see Fig. 3). The χ_{KPZ} s listed in Table 1 show that that our numerical χ_{KPZ} s are in close agreement with Medina et al.'s [11] and Chattopadhyay and Bhattacharjee's [12] theoretical results. Our results are consistent with earlier simulations by Amar et al. [16], Peng et al. [15], and Meakin and Julien [17,18]. For $\rho = 0.75$ Hayot and Jayaprakash [3] have reported a crossover in the wave number space—from RG dominated region for small k to shock dominated region for large k . We do not find any such crossover in our simulation. Regarding the Burgers equations, $\chi_{Burg} = \chi_{KPZ} - 1$.

Regarding β_{KPZ} calculations, our results are agreement with Medina et al.'s predictions for $\rho = 0 - 0.25$. However, our exponents differ significantly with Medina et al.'s exponents for higher ρ s. For example, for $\rho = 1$, we obtain $\beta_{KPZ} = 0.45$ contrary to the predicted $\beta_{KPZ} = 1$. The reason for this discrepancy is not clear to us at this point. Regarding β_{Burg} , we find that it is approximately 0.5, consistent with Hayot and Jayaprakash's findings [3]. Theoretical arguments in support of $\beta_{Burg} \approx 0.5$ is lacking.

B. $\rho > 5/2$

One of the important aspect of this paper is the solution of KPZ equation for large ρ . Table 1 and Fig. 3 shows that the exponent $\chi_{KPZ} \approx 3/2$ for $\rho > 5/2$. Note that $\chi_{KPZ} = 3/2$ and $\chi_{Burg} = 1/2$ for the noiseless Burgers equation. This gives us a clue that the shocks appear for large ρ . It can be verified by looking at $u(x, t)$. Fig. 4 shows numerical $u(x, t)$ for various ρ s. The plot clearly shows the presence of shock-like structures for $\rho = 3, 7$ (compare with Fig. 1).

The existence of shocks for large ρ can be argued from the noise-noise correlation discussed in the early part of this section. For large ρ , there are long-ranged noise-noise correlations. Physically, large fluid parcels are moved around by this noise. As shown in Fig. 4, there are regions where the parcels forced by appositely directed noise collide with

each other and create “strong” shocks. Hence, it is not surprising that strong shocks are generated for large ρ . These shocks determine the dynamics and the spectral indices of Burgers and KPZ equations. Therefore, the noisy KPZ equation with large ρ yields the same spectral exponent as the noiseless KPZ equation. Similar results are borne out by multiscaling studies which will be reported in paper II.

The noise-noise correlation is proportional to $1 - Cr^2$ for all $\rho \geq 5/2$, hence the spectral and multiscaling exponents are expected to somewhat similar to all the ρ beyond $5/2$. This is borne out by our numerical simulation. Also, only $k = 1$ mode is effective for large ρ . It is interesting to observe that $k = 1$ mode (i.e., $\zeta(x) = \sin(x)$) also gives correlation proportional to $1 - Cr^2$. We find that the exponents for single forcing mode is approximately the same as that by any correlated noise beyond $\rho = 5/2$.

We have also analyzed the stability of the shocks at a preliminary level. For large ρ , the significant contribution to the dynamics comes only from the $k = 1$ mode of the noise. Since the first mode ($k = 1$) is noisy, the the formation of a single shock occurs after some time because of the movement of the zero of the noise signal. However, after the shock is formed, it shifts around by only a small amount. This is because the impulse due to the random noise is not strong enough to move the shock by a large distance.

We have also calculated β for both Burgers and KPZ equations when $\rho > 5/2$ and find them to be approximately $1/2$. This result is consistent with findings of Hayot and Jayaprakash [3]. The analytic reasoning behind $\beta \approx 0.5$ is not known.

C. $1 \leq \rho \leq 2$

The χ_{KPZ} calculated by our numerical simulation for the range $1 \leq \rho \leq 5/2$ is listed in Table 1. The exponent increases from 1 and saturate at $3/2$. That is, there is a gradual shift from RG dominated exponents to shock dominated exponents as we vary ρ . The profile $u(x, t)$ shown in Fig. 4 shows that both fluctuations and shocks coexist in this range, with shocks becoming more and more important as ρ increases. For this range of ρ we do not have any analytic result in order to obtain the energy spectrum. We presume that both fluctuations and the embedded structures are important in the determination of the spectral index. One would need to the combined contribution from the structures and fluctuations to obtain the energy spectrum [25,26]. In Appendix B we sketch an elementary framework when both structure and fluctuations are present in the system.

The Burgers equation for $\rho = 3/2$ has been studied extensively by Chekhlov and Yakhot [1]. They find in their large resolution simulation that $|u(k)|^2 \propto k^{-5/3}$. The spectrum in our low resolution simulation is $|u(k)|^2 \propto k^{-1.54}$ ($\chi_{KPZ} = 1.27$), which is close to Chekhlov and Yakhot’s [1] result. Chekhlov and Yakhot [1] have argued for a constant cascade of energy in the wavenumber space in this case and claimed that the Kolmogorov-like energy spectra is due to the constancy of the energy flux. However, we find the cascade rate to be constant for all $\rho > 1.5$, but the spectral indices of the energy spectrum is in the range of $5/3$ to 2 (to be discussed in Section 5). Hence, the argument that the constant flux yields Kolmogorov’s spectrum is suspect.

From the above discussion we see that Burgers and KPZ equations are well understood for $0 \leq \rho \leq 1$ and $\rho > 5/2$. In the intermediate range $1 < \rho < 5/2$, analytic results are not available, yet it is clear that structures and fluctuations both play important role in the statistical analysis.

For all $\rho > 1/2$, $\chi_{KPZ} + z$ ($z = \chi_{KPZ}/\beta_{KPZ}$) deviates significantly from 2. In fact, for larger ρ , $\chi_{KPZ} + z = 3/2 + (3/2)/(1/2) = 9/2$, quite far from 2. Note that Medina et al. [11] argue that the identity $\chi_{KPZ} + z = 2$ as a consequence of Galilian invariance. However, Hayot and Jayaprakash [3], Polyakov [2] and others have speculated violation of this identity due to presence and motion of the shocks. Meakin and Jullien’s [17,18] results also violate $\chi_{KPZ} + z = 2$ condition for large ρ . They find that for $\rho = 0.75$, $\chi_{KPZ} + z = 2.37$. For $\rho = 1$, the exponents have not been reported in their paper. The violation of Galilian invariance even in the region $0 \leq \rho \leq 1$ signals importance of structures [2].

The energy flux play an in important role in turbulence analysis. In the following section we report energy flux studies for the Burgers equation.

V. ENERGY FLUX OF NOISY BURGERS EQUATION

We derive an equation which gives us the energy transfer from the region $|k| \leq K$. The derivation of the energy equation from Eq. (I) and averaging yields [27]

$$\frac{\partial}{\partial t} \int_0^K E(k) dk = - \int_0^K 2\nu k^2 E(k) dk - \int_0^K \Re \langle u^*(k) \left[FT \left(\frac{\partial}{\partial x} u^2/2 \right) \right]_k \rangle + \int_0^K \Re \langle u^*(k) f(k) \rangle. \quad (5.1)$$

From this equation, clearly the energy dissipation in the wavenumber sphere of radius K is

$$D_K = \int_0^K 2\nu k^2 E(k) dk, \quad (5.2)$$

and the energy flux coming out the wavenumber sphere of radius K is

$$\Pi_k = \int_0^K \Re \langle u^*(k) \left[FT \left(\frac{\partial}{\partial x} u^2/2 \right) \right]_k \rangle. \quad (5.3)$$

It can easily be seen that for the random noise, the energy supplied by the forcing to the wavenumber sphere of radius K is [27]

$$\begin{aligned} F_K &= \int_0^K \Re \langle u^*(k) f(k) \rangle \\ &= \int_0^K \langle |f(k)|^2 \rangle. \end{aligned} \quad (5.4)$$

From the Eq. (5.1) it is clear that at the steady state

$$F_K = \Pi_K + D_K. \quad (5.5)$$

We have plotted D_K , Π_K , and F_K for various ρ . Fig. 5 shows the plots for $\rho = 1$. Here, we find that $D_K \approx F_K$ till $k \approx 250$, but $\Pi_K \ll F_K$ except for small k . Similar results are obtained for all $0 \leq \rho \leq 1$.

Fig. 6 shows the plots of D_K , Π_K , and F_K for $\rho = 1.5$. The forcing rate F_K is proportional to $\log(K)$. We also find a range of K for which Π_K is constant. These results are consistent with the findings of Chekhlov and Yakhot [1]. Fig. 7 shows a generic plot of the above quantities for $\rho = 7$. Here again Π_K is constant for a range of K . An interesting point to note is that for $\rho = 7$, F_K is constant beyond $K = 10$ or so; this is because effectively only first few modes are forced when ρ is large. Similar results are obtained for all $\rho \geq 2$.

We find that the energy flux is constant for the noisy Burgers equation for all $\rho \geq 3/2$. However, the energy spectrum varies from $k^{-5/3}$ to k^{-2} as we increase ρ from $3/2$ to 2 and beyond. Hence our results show that constancy of energy flux is not a sufficient condition for the Kolmogorov's energy spectrum in noisy Burger equation. This indicates that the arguments of Chekhlov and Yakhot [1] is not complete.

We find that for $\rho \geq 2$, the flux rate $\Pi_K \approx 2 \times 10^{-3}$. This numerical value is consistent with value obtained using the formula derived by Saffman [28]

$$\Pi_K \approx \frac{\mu^3}{24L}, \quad (5.6)$$

where μ is the velocity jump across the shock. In our simulations, $\mu \approx 0.3$ for large ρ . Also, the Eq. (5.4) yields the same numerical value ($2D = 2 \times 10^{-3}$).

VI. DISCUSSION AND CONCLUSIONS

In this paper we have numerically calculated the energy spectrum for KPZ and Burgers equations in the presence of correlated noise. The Burgers equation with a strong correlated noise ($\rho \geq 5/2$) has distinct shock structures. Given this we have trivially worked out the roughening exponents for this range: $\chi_{Burg} = 1/2$, $\chi_{KPZ} = 3/2$ and $\beta = 1/2$. The small ρ regime ($0 \leq \rho \leq 1$, "weakly" correlated noise) has weak structures or no structure, therefore, fluctuations dominate. As a consequence RG is expected to work in this regime. For this range of ρ our numerical results are consistent with the RG results of Medina et al. [11].

For $1 \leq \rho \leq 5/2$ we find that the velocity profile has shock structures embedded in the fluctuation. Therefore, the roughening exponent will get contributions both from fluctuations and embedded structures. We believe careful analysis is required to isolate the individual contributions. Krishnamurthy and Barma [25,26] have isolated a moving pattern in the surface growth phenomena in the presence of quenched disorder. Their analysis may be applied here to separate the fluctuations from the structures, however, their method based on lattice simulations is not easy to implement in spectral or finite element method.

In this paper we have demonstrated the usefulness of structures in calculating the dynamical exponents of the system. The role of structures in dynamics is being studied in fluid turbulence, intermittency, self organized criticality etc. For example, in fluid turbulence Hatakeyama and Kambe [29] have used the vortex structures to calculate the scaling exponents. Therefore, discovery of the connections between the structures, fluctuations, and dynamics will yield interesting insights in the nonequilibrium phenomena around us.

ACKNOWLEDGMENTS

The author thanks Mustansir Barma, Supriya Krishnamurthy, and Deepak Dhar for discussions, references, and their kind hospitality during his stay at TIFR, where part of this work was done. V. Subrahmanyam's ideas and criticisms are gratefully acknowledged. The author also thanks J. K. Bhattacharjee, Agha Afsar Ali, and Prabal Maiti for discussions at various stages, and R. K. Ghosh for providing computer time on DEC workstation.

APPENDIX A: EFFECTS OF PARAMETERS

The roughening exponents of KPZ equation are stated without reference to the range of the parameter values. Usually it is assumed that ν is small. This is in the same spirit as in fluid turbulence. While performing our simulations for nonzero ρ we, however, found interesting changeover in the behaviour of KPZ even when ν was small. We describe our findings below.

As discussed in the main text, for the parameter described in Eq. (3.1), we get the exponents shown in Table 1. However, in one of the test runs we fixed ν at a somewhat higher value $\nu = 0.05$, and chose $D = 0.001$. For these parameters we found a transition from $k^{-2\rho-2}$ to $k^{-2\rho}$ and finally to $k^{-\chi_{KPZ}}$, where χ_{KPZ} is given in Table 1. To understand this transition, we need to look at the energy spectrum of Edward-Wilkinson (EW) and Random deposition (RD) models.

EW equation is given by

$$\frac{\partial h(x, t)}{\partial t} = \nu \nabla^2 h(x, t) + f(x, t). \quad (\text{A1})$$

The above equation can be solved easily in Fourier space, which yields

$$h(k, \omega) = \frac{f(k, \omega)}{i\omega - \nu k^2}. \quad (\text{A2})$$

Using

$$\langle f(k, \omega) f(k', \omega') \rangle = 2D \frac{k^{-2\rho}}{i(\omega - \omega')}. \quad (\text{A3})$$

we can easily show that

$$\langle h(k, t) h^*(k, t) \rangle = k^{-2\rho-2} (A + B \exp(-2\nu k^2 t)) \quad (\text{A4})$$

Therefore, EW equation at large t yields $|h(k)|^2 \propto k^{-2\rho-2}$.

If we substitute $\nu = 0$ in the Eq. A1, we obtain the Random deposition (RD) model [23] which is

$$\frac{\partial h(x, t)}{\partial t} = f(x, t). \quad (\text{A5})$$

Using a similar procedure as above, we obtain $|h(k)|^2 \propto k^{-2\rho}$ for this equation.

Now we can explain the crossover from EW to RD and then to KPZ behaviour. In the initial phase, the width $\langle h^2 \rangle$ is small, hence the viscous term dominates both noise and nonlinear term, consequently EW behaviour is seen. As time progress and the width increases, the noise term becomes dominant and RD behaviour is observed. In this regime the width increases linearly in time [23]. At a later time when the width become large enough, the nonlinear term takes over, and KPZ like behaviour is observed. This is the reason why the spectral index varies from EW to RD to KPZ regimes.

Our findings regarding the crossover from EW to KPZ etc. show that we should be careful in choice of parameters while simulating KPZ and Burgers equations.

APPENDIX B: EXPONENTS WHEN BOTH STRUCTURES AND NOISE ARE PRESENT

A surface profile $h(x)$ can be split into two parts:

$$h(x) = h_s(x) + h_f(x), \quad (\text{B1})$$

where $h_f(x)$ denotes the fluctuation, and $h_s(x)$ denotes the embedded structure. By definition, $\langle h_f(x) \rangle = 0$ where $\langle \cdot \rangle$ denotes the ensemble average. Therefore, $\langle h(x) \rangle = h_s(x)$.

We can show that the width squared W^2 , which is obtained by taking the spatial average, is

$$\begin{aligned} W^2 &= \overline{\langle (h(x) - \bar{h})^2 \rangle} \\ &= W_s^2 + W_f^2 \end{aligned} \quad (\text{B2})$$

Hence, W^2 is the sum of the contributions from the fluctuating part and the structure part. Similarly, the second-order structure function $T_2(r)$ is the sum of two contributions,

$$\begin{aligned} T(r) &= \overline{\langle |h(x+r) - h(x)|^2 \rangle} \\ &= T_s(r) + T_f(r). \end{aligned} \quad (\text{B3})$$

Hence, in a profile with an embedded structure, the exponent is determined by both structure and fluctuations.

There is no structure in KPZ profile for $\rho = 0$, hence, the roughening exponent is totally determined by the fluctuations. However, the profile for the noiseless Burgers equation has only shock structure, which determines the roughening exponent. In KPZ equation with correlated noise, especially for $1 < \rho < 5/2$, we have both structure and fluctuations. Therefore, we will have to do a careful analysis combining both of them to obtain the roughening exponents for these cases. We expect that similar analysis has to be carried out for the surface growth profile with quenched disorder that has both structure and fluctuations.

- [1] A. Chekhlov and V. Yakhot, Phys. Rev. E **51**, R1 (1995).
- [2] A. M. Polyakov, Phys. Rev. E **52**, 6183 (1995).
- [3] F. Hayot and C. Jayaprakash, Phys. Rev. E **54**, 4681 (1996).
- [4] M. K. Verma, preprint (1999).
- [5] S. Kida, J. Fluid Mech. **93**, 337 (1979).
- [6] T. Gotoh, Phys. Fluids A **6**, 3985 (1994).
- [7] J. P. Bouchaud, M. Mézard, and G. Parisi, Phys. Rev. E **52**, 3656 (1995).
- [8] J. M. Burgers, *The Nonlinear Diffusion Equation* (Reidel, Boston, 1974).
- [9] T. Tatsumi and S. Kida, J. Fluid Mech. **55**, 659 (1972).
- [10] M. Kardar, G. Parisi, and Y.-C. Zhang, Phys. Rev. Lett. **56**, 889 (1986).
- [11] E. Medina, T. Hwa, and M. Kardar, Phys. Rev. A **39**, 3053 (1989).
- [12] A. K. Chattopadhyay and J. K. Bhattacharjee, Europhys. Lett. **42**, 119 (1998).
- [13] Y.-C. Zhang, Phys. Rev. A **42**, 4897 (1990).
- [14] H. G. E. Hentschel and F. Family, Phys. Rev. Lett. **66**, 1982 (1991).
- [15] C.-K. Peng, S. Havlin, M. Schwartz, and H. E. Stanley, Phys. Rev. A **44**, R2239 (1991).
- [16] J. G. Amar, P.-M. Lam, and F. Family, Phys. Rev. A **43**, 4548 (1991).
- [17] P. Meakin and R. Jullien, Europhys. Lett. **9**, 71 (1989).
- [18] P. Meakin and R. Jullien, Phys. Rev. A **41**, 983 (1990).
- [19] M. J. Lighthill, *Introduction to Fourier Analysis and Generalised Functions* (Cambridge University Press, Cambridge, 1959).
- [20] C. Canuto, M. Y. Hussaini, A. Quarteroni, and T. A. Zhang, *Spectral Methods in Fluid Turbulence* (Springer-Verlog, Berlin, 1988).
- [21] K. Moser, J. Kertész, and D. E. Wolf, Physica A **178**, 215 (1991).
- [22] M. K. Verma *et al.*, J. Geophys. Res. **101**, 21619 (1996).
- [23] A.-L. Barabasi and H. E. Stanley, *Fractal Concepts in Surface Growth* (Cambridge University Press, New York, 1995).
- [24] W. H. Press, B. P. Flannery, S. A. Teukolsky, and W. T. Vetterling, *Numerical Recipes in C*, 2 ed. (Cambridge University Press, Cambridge, 1992).
- [25] S. Krishnamurthy and M. Barma, Phys. Rev. Lett. **76**, 423 (1996).
- [26] S. Krishnamurthy and M. Barma, Phys. Rev. E **57**, 2949 (1998).
- [27] W. D. McComb, Phys. Rev. A **26**, 1078 (1982).
- [28] P. G. Saffman, in *Topics in Nonlinear Physics*, edited by N. J. Zabusky (Springer, Berlin, 1968), pp. 485–614.
- [29] N. Hatakeyama and T. Kambe, Phys. Rev. Lett. **79**, 1257 (1997).

Figure Captions

Fig. 1 The solutions of noiseless Burgers and KPZ equations.

Fig. 2 The width $\langle |h(x) - \langle h \rangle|^2 \rangle^{1/2}$ vs. t for $\rho = 0.0$. Saturation occurs at around $t = 8$. The curve of best fit $W^2 = 0.07 * t^{0.70}$ for $t = 0 : 2.5$ is shown in the Figure.

Fig. 3 The energy spectrum $(1/2) \langle |h(k)|^2 \rangle$ vs. k for the KPZ equation when $\rho = 0, 1, 1.5, 3$. The lines of best fit for the intermediate range of k are also shown.

Fig. 4 The normalized velocity profile $u(x)$ vs. x for Burgers equation when $\rho = 0, 1/2, 1, 3/2, 2, 3, 7$. The profile is noisy for $0 \leq \rho \leq 1$, has only well developed shocks for $\rho > 5/2$, and has both fluctuations and shocks for the intermediate range.

Fig. 5 The Dissipation rate D_K , the energy flux Π_K , and the forcing rates F_K vs. K for $\rho = 1$.

Fig. 6 The Dissipation rate D_K , the energy flux Π_K , and the forcing rates F_K vs. K for $\rho = 3/2$.

Fig. 7 The Dissipation rate D_K , the energy flux Π_K , and the forcing rates F_K vs. K for $\rho = 7$.

TABLE I. The exponents α and β for KPZ equation for various ρ 's. The Medina et al.'s exponents are also listed for comparison.

ρ	Our results		Medina et al.'s results	
	α	β	α	β
0.00	0.46	0.35	0.50	0.33
0.15	0.50	0.28	0.50	0.33
0.25	0.53	0.31	0.50	0.33
0.40	0.60	0.33	0.60	0.43
0.50	0.70	0.36	0.67	0.50
0.75	0.89	0.42	0.83	0.71
1.00	1.07	0.45	1.00	1.00
1.50	1.27	0.48		
2.00	1.58	0.48		
3.00	1.54	0.48		
7.00	1.45	0.48		

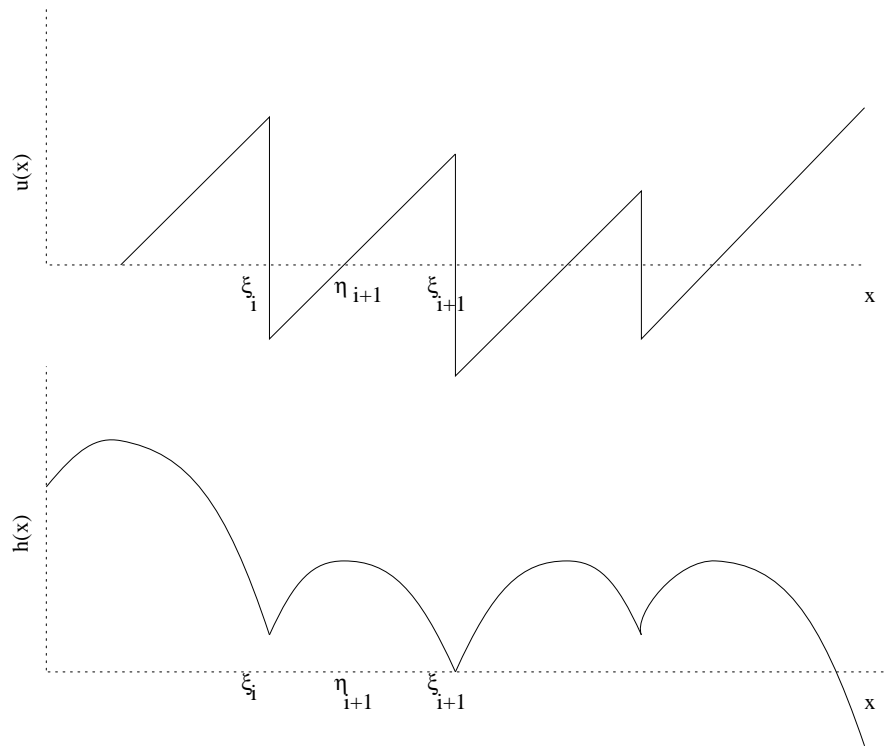


FIG. 1.

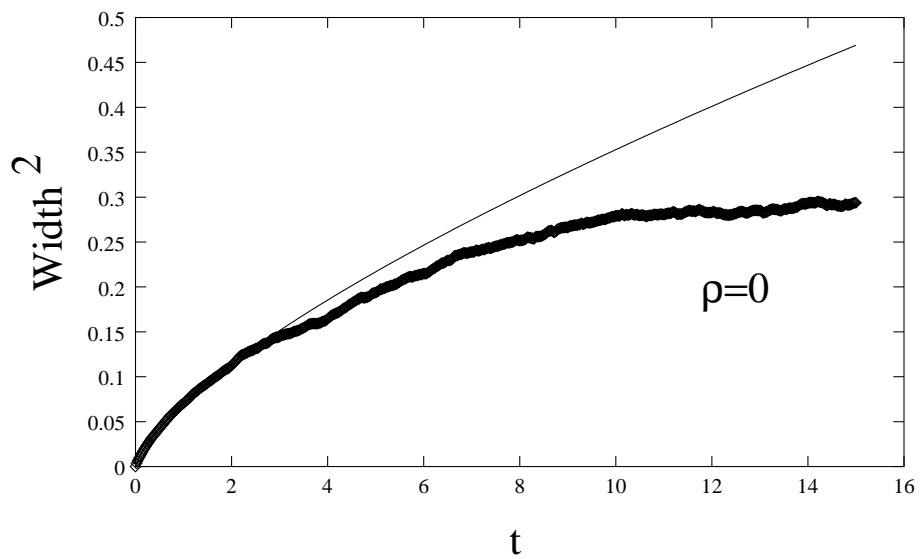


FIG. 2.

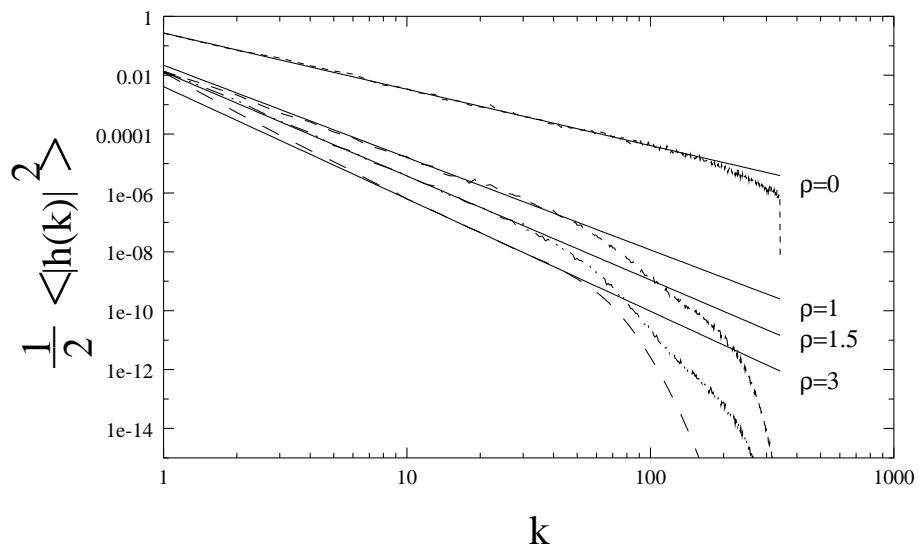


FIG. 3.

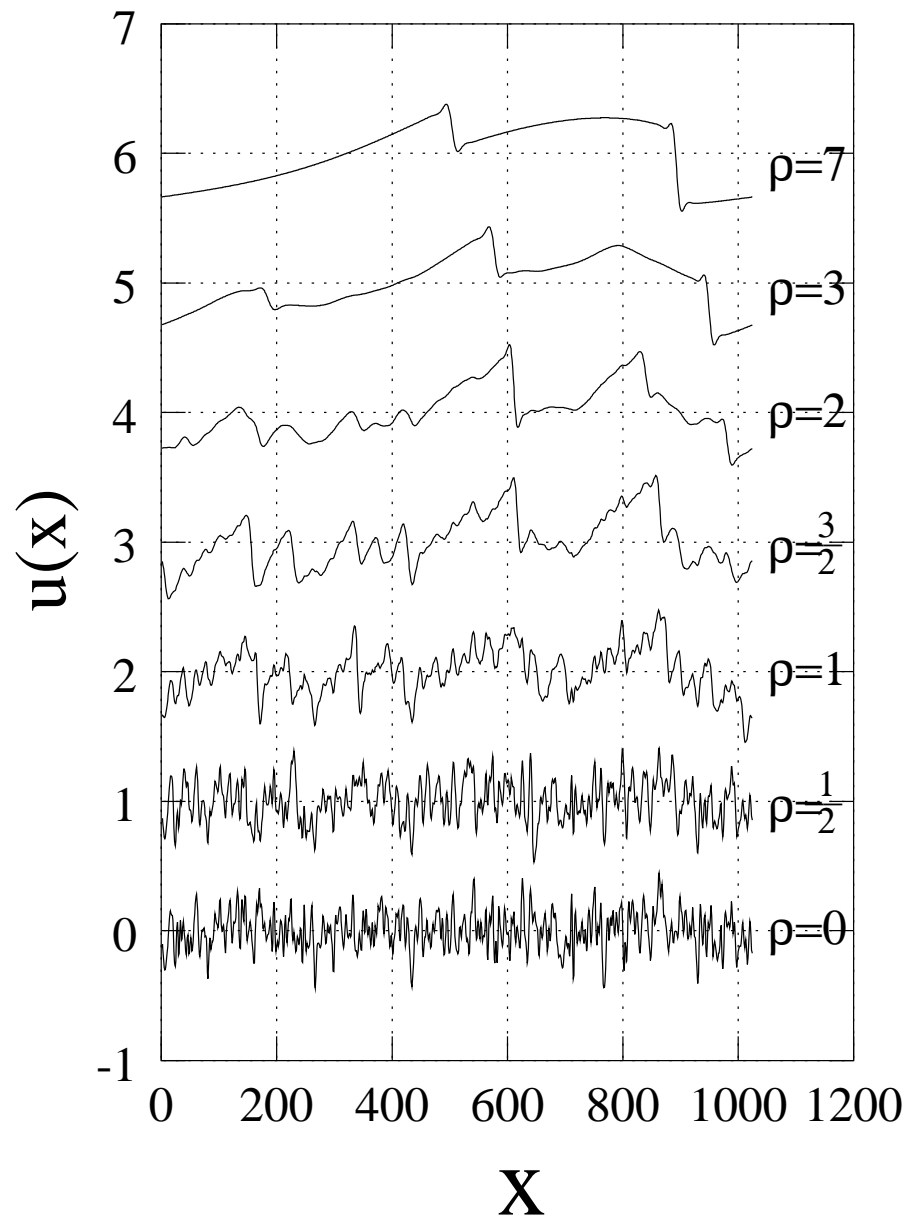


FIG. 4.

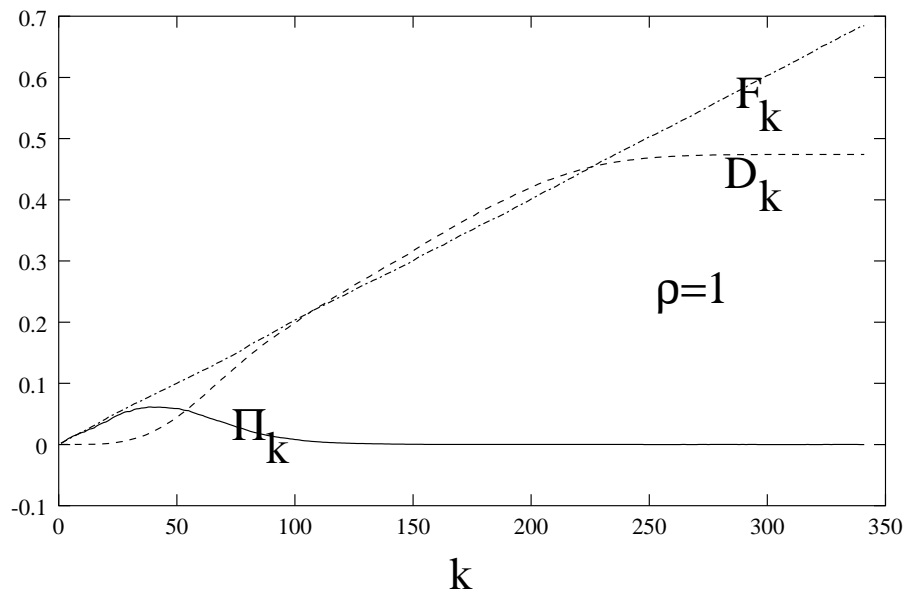


FIG. 5.

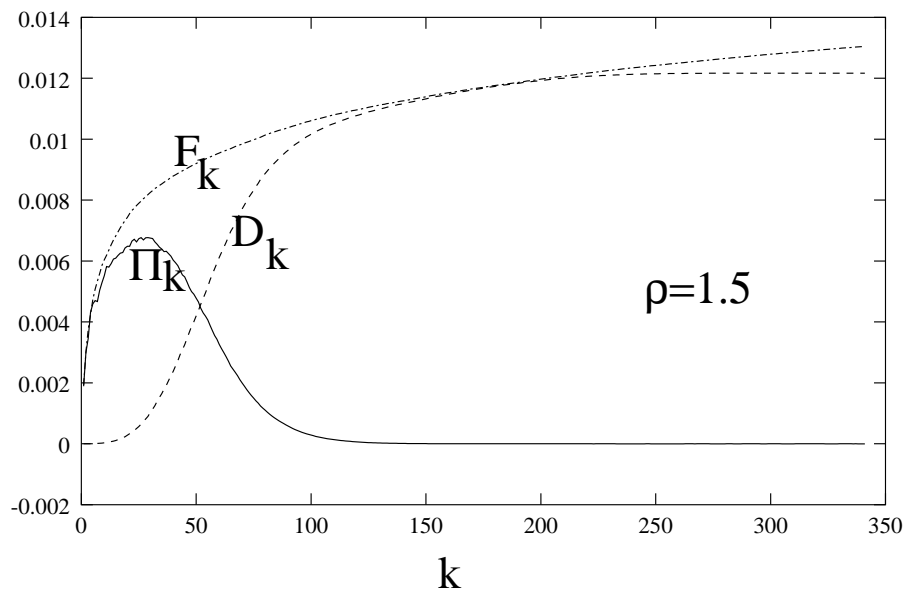


FIG. 6.

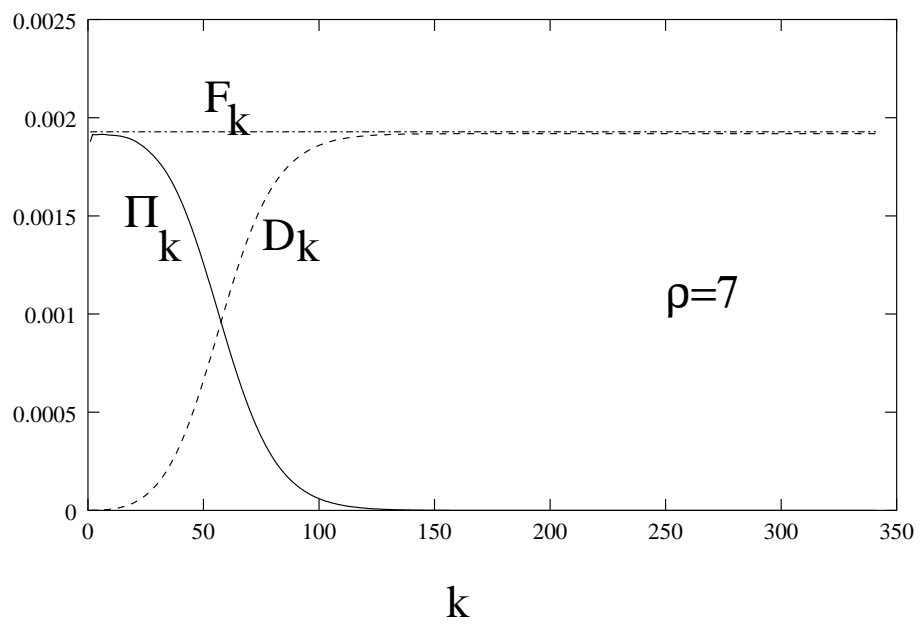


FIG. 7.